Title

Evidence for cis Amide Bonds in Peptoid Nanosheets

Journal

The Journal of Physical Chemistry Letters, 9(10)

ISSN

1948-7185

Authors

Hudson, Benjamin C

Battigelli, Alessia

Connolly, Michael D

et al.

Publication Date

2018-05-17

DOI

10.1021/acs.jpclett.8b01040

Peer reviewed

Evidence for cis Amide Bonds in Peptoid Nanosheets

Benjamin C. Hudson[†], Alessia Battigelli[‡], Michael D. Connolly[‡], John Edison[‡], Ryan K. Spencer[‡], Stephen Whitelam[‡], Ronald N. Zuckermann*[,‡], and Anant K. Paravastu*[,†]

[†]Department of Chemical and Biomolecular Engineering, Georgia Institute of Technology, Atlanta, Georgia 30332-0100, United States

[‡]Molecular Foundry, Lawrence Berkeley National Laboratory, Berkeley, California 94720, United States

Supporting Information Placeholder

ABSTRACT: Peptoid nanosheets are supramolecular protein-mimetic materials that form from amphiphilic polypeptoids with aromatic and ionic sidechains. Nanosheets have been studied at the nanometer scale, but molecular structure has been difficult to probe. We report the use of ^{13}C-^{13}C dipolar recoupling solid-state NMR measurements to reveal the configuration of backbone amide bonds selected by ^{13}C isotopic labeling of adjacent α-carbons. Measurements on the same molecules in the amorphous state and in nanosheets revealed that amide bonds in the center of the amino block of peptoid $(NaeNpe)_7$-$(NceNpe)_7$ (B28) favor the *trans* configuration in the amorphous state and the *cis* configuration in the nanosheet. This unexpected result contrasts with previous NMR and theoretical studies of short solvated peptoids. Furthermore, examination of the amide bond at the junction of the two charged blocks within B28 revealed a mixture of both *cis* and *trans* configurational states, consistent with the previously-predicted brickwork-like intermolecular organization.

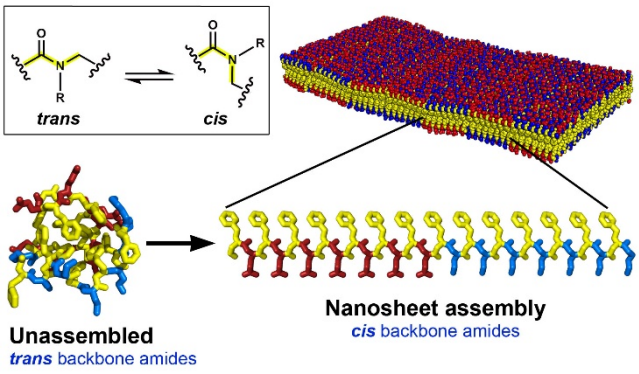

Peptoids are peptide-mimetic sequence-defined heteropolymers that can form highly ordered crystals in the solid state and protein-like supramolecular assemblies in aqueous solution [1-3]. Their folding and assembly are influenced by the sequence of chemically diverse sidechains along an *N*-substituted glycine backbone. Peptoid residues are polymerized iteratively with precise sequence control via solid-phase synthesis techniques that are analogous to peptide synthesis techniques [4]. Peptoid nanosheets are of particular interest because they have highly uniform bilayer structures, are free-floating in water, and are biocompatible. Nanosheets can serve as affinity reagents and templates for the growth of composite materials, and hold great potential for use as membranes for separations and as a platform for chemical and biological sensing [4]. Motivated by structural similarities between peptoids and peptides, one fundamental goal in the field of biomimetic chemistry is to create well-defined, folded tertiary structures that mimic the architecture, and ultimately the function, of proteins [5].

In this work, we took advantage of similarities between peptoid and peptide chemistry in order to answer a long-standing structural question about peptoids. This question is related to the configuration of backbone amide bonds (torsion angle ω). Double bond character results in two possible values for ω. For peptides, *cis* amide bonds (ω = 0) are rare and *trans* (ω = 180°) is the favored configuration. For peptoids, theoretical calculations suggest that trans remains the favored configuration, but the energy gap between *trans* and *cis* amide bonds (see Figure 1A and 1B) is reduced by the attachment of sidechains to backbone N atoms (peptide sidechains connect to Cα atoms) [6]. Thus, the theoretical calculations and solution NMR measurements suggested that, despite the smaller energy gap, there would be no effect on backbone amide configurational distributions [6, 7]. Using solid-phase synthesis techniques, we produced peptoid $(NaeNpe)_7$-$(NceNpe)_7$ (B28) (Figure 1C) samples with precise incorporation of ^{13}C isotopic labels at selected pairs of adjacent Cα sites (see Figure S1). The accessibility of this isotopic labeling made it possible for us to employ solid-state NMR dipolar recoupling measurements in order to probe the relative abundance of *cis* and *trans* amide bonds in peptoid B28 samples. Isomerization of the amide bond was expected to affect the distance between adjacent Cα sites and therefore the strength of ^{13}C-^{13}C magnetic dipolar couplings [8].

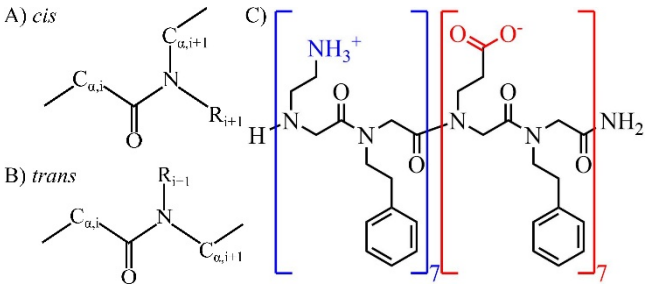

Figure 1. A) and B) Planar representations of a backbone peptoid amide bond in the *cis* and *trans* configurations, respectively. C) Primary structure of peptoid B28 with the positively charged amino block colored in blue and the negatively charged carboxylic acid block colored in red.

The 28-residue B28 peptoid self-assembles into stable nanosheets (Figure 2) and is representative of sidechain patterning of nanosheet-forming peptoids [9]. Counting from the amino terminus, the 14 even numbered residues in B28 are hydrophobic *N*-(2-phenylethyl)glycine (Npe) units. The first 7 odd numbered monomers are cationic (at neutral pH) *N*-(2-aminoethyl)glycine (Nae) units, such that the first half of the B28 molecule would be considered a positively charged block. The odd numbered sidechains on the second half of the molecule are anionic *N*-(2-carboxyethyl)glycine (Nce) units, resulting in a negatively charged block. This alternating sequence motif of aromatic and ionic monomers is quite general for nanosheet formation, enabling functionalization and structural engineering of nanosheets for a variety of applications [4]. For peptides, such an alternation would promote β-strand conformation, which would place aromatic and ionic sidechains on opposite faces of an amphiphilic molecular conformation [10]. Peptoid nanosheets are believed to be composed of molecules in analogous amphiphilic extended conformations. Furthermore, the organization of ionic sidechains to produce like-charged blocks is believed to promote a brickwork-like inter-molecular organization [9]. This structure contrasts with β-sheet nanofiber structures formed by peptides such as RADA16-I, which are composed of chiral amino acid subunits, have backbone conformations characterized by a single rotational state, and form supramolecular structures that extend in only one dimension (nanofibers rather than nanosheets).

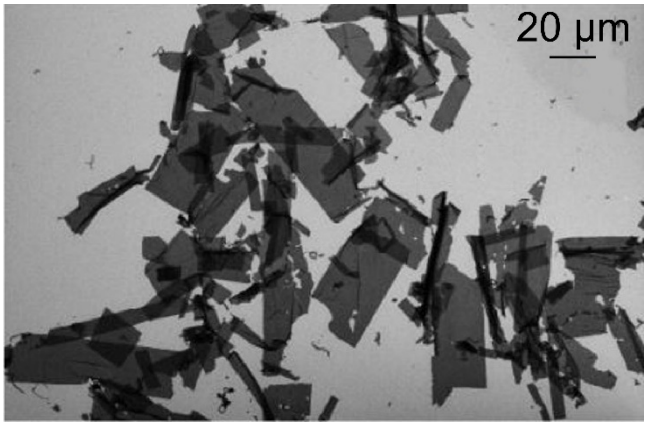

Figure 2. Transmission electron microscopy image of peptoid B28 nanosheets.

Previous experimental reports on peptoid nanosheet structure have primarily focused on the nanoscale order, using x-ray scattering, atomic force microscopy, and transmission electron microscopy [1]. In order to probe the atomic-level details of the backbone conformation, it is essential to use higher resolution spectroscopic techniques like those based on solid-state NMR. Solid-state NMR techniques have recently been used successfully to elucidate the molecular structure of an analogous peptidic material, amyloid fibrils formed by RADA16-I [10]. More broadly, solid-state NMR techniques have contributed to our understanding of biological and non-biological supra-molecular assembles, particularly those that are incompatible with purely crystallographic techniques [11-18]. Dipolar recoupling NMR measurements have been of unique significance because they produce observables that can be interpreted quantitatively in terms of inter-atomic distances [8, 19].

Recent molecular-dynamics simulations of peptoid B28 nanosheets revealed that peptoid polymers can form a flat, extended molecular conformation by adopting a proposed form of secondary structure called a ∑-strand [9]. Analogous to the peptide β-strand, the ∑-strand is a confirmation in which adjacent residues in the peptoid backbone adopt twist-opposed rotational states, allowing the polymer as a whole to remain linear and untwisted. For the ∑-strand, backbone amide bonds are in the *trans* configuration. To predict the distribution of distances between adjacent Cα sites in this conformation, molecular dynamics simulations on single B28 ∑-strands were performed. Additional simulations were performed on peptoid B28 molecules with amide bonds in the *cis* configuration. Resultant distance distributions are shown in Figure 3.

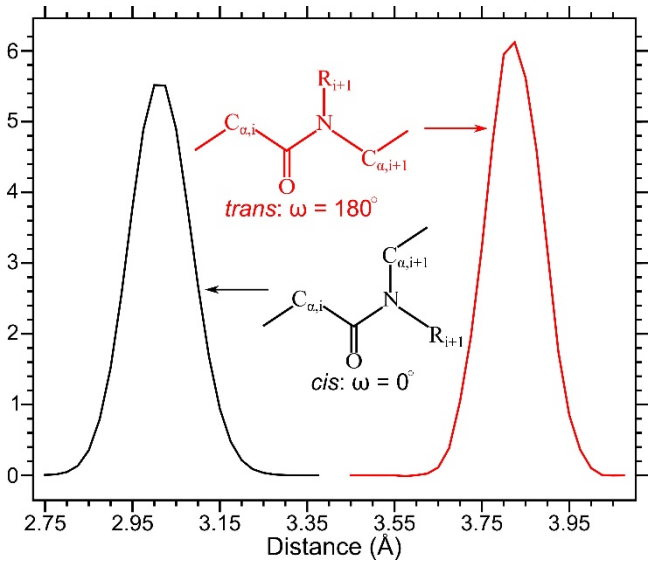

Figure 3. Comparison of *cis* and *trans* configurations and their respective Cα-Cα distance distribution estimates from molecular dynamics simulations of peptoid B28 monomer units (single molecules).

To probe the isomerization state of B28 backbone amide bonds, we employed PITHIRDS-CT dipolar recoupling solid-state NMR on samples that were isotopically labeled with ^{13}C at pairs of adjacent Cα sites. We examined the dependence of measured ^{13}C PITHIRDS-CT NMR peak intensity on ^{13}C-^{13}C dipolar evolution time (Figure 4). Samples were ^{13}C-labeled at residues 6 and 7, 7 and 8, or 14 and 15 (see Figure 4A). For each ^{13}C labeled pair, experiments were performed on a nanosheet sample, and an unassembled, amorphous control sample for a total of 6 samples. The ^{13}C NMR spectra of these samples are shown in Figures S3, S4, and S5. The nanosheet spectral line widths are consistent with ordered molecular arrangement, and it is clear that a structural transition has occurred between the amorphous control and nanosheet samples. Nanosheet samples were assembled using a scaled up vial rocking method [4], and the amorphous samples were obtained from lyophilization of the B28 peptoid from acetonitrile/water (1:1, v/v). Each data point represents the integrated intensity of measured NMR signal for a specific evolution time under the influence of ^{13}C-^{13}C magnetic dipolar coupling (estimated error based on NMR signal-to-noise is on the order of the symbol size). Data were corrected for the expected contribution of 1% naturally abundant ^{13}C background signal corresponding to unlabeled aliphatic sites in B28.

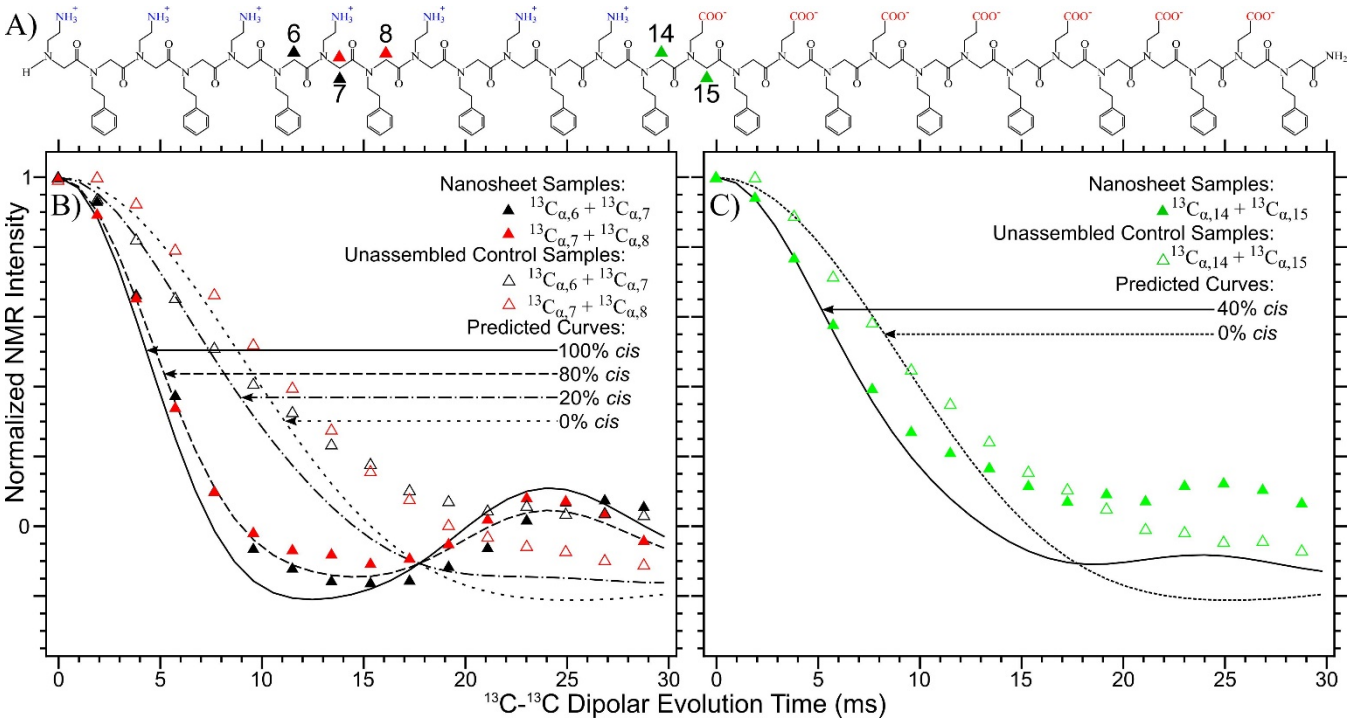

Figure 4. A) Unabbreviated primary structure of peptoid B28 with ^{13}C-labeled Cα pairs identified by black triangles (6, 7), red triangles (7, 8), and green triangles (14, 15). B) PITHIRDS-CT data for Cα pairs (6, 7) and (7, 8). Nanosheet (*cis*) decays are indicated by filled triangles, and amorphous control (*trans*) decays are indicated by empty triangles. C) PITHIRDS-CT decays from nanosheet (filled triangles) and amorphous control samples (empty triangles) labeled at (14, 15). Color scheme for (B) and (C) is maintained from (A). Simulated curves are shown to indicate predicted PITHIRDS-CT decays for distance distributions corresponding to 100% *cis*, 80% *cis*, 20% *cis*, and 0% *cis* in (B) and 40% *cis*, and 0% *cis* in (C).

Nuclear spin simulations were performed using SPINEVOLUTION™ [20] in order to quantify the dependence of PITHIRDS-CT decay on interatomic distance for a pair of ^{13}C nuclei. The theoretical curves shown in Figure 4 are the sums of simulated NMR decays, weighted in terms of distributions of predicted ^{13}C-^{13}C distances in Figure 3. All three amorphous control samples exhibit similar decay curves (empty symbols in Figure 4A and 4B), indicative of a primarily *trans* amide bond population. In contrast, measured decays for nanosheet samples labeled at residues 6 and 7 and residues 7 and 8 (Figure 4A, filled symbols) are consistent with a predominantly *cis* configuration. Data from the nanosheet samples labeled at positions 14 and 15 (Figure 4B, filled symbols) indicate a more even split in the population with an estimated 40% contribution of the *cis* configuration. Potential effects of inter-molecular ^{13}C-^{13}C dipolar couplings were considered using spin simulations (Figure S2) and we determined that the strongest possible intermolecular ^{13}C dipolar couplings would not affect our assessment of *trans* versus *cis* amide bonds.

The PITHIRDS-CT results in Figure 4 have important implications. Results for amorphous control samples are harmonious with previous experimental analyses on small, solvated peptoid molecules and theoretical predictions that suggest a lower energy for *trans* amide bonds [6, 7]. However, here we experimentally observe, for the first time, that peptoid B28 nanosheets appear to exhibit significant contribution from the *cis* configuration at multiple backbone amide bonds. As we see it, our results motivate two possible explanations that are not necessarily mutually exclusive. First, that the energetics of intermolecular interactions occurring during self-assembly could be sufficiently strong to promote isomerization of amide bonds from *trans* to *cis*, likely due to enthalpic gains from inter-molecular sidechain interactions. Second, isomerization from *trans* to *cis* could occur prior to self-assembly. If this were true, it would likely indicate that the *cis* configuration increases the propensity for nanosheet assembly, given the results supporting *cis*-dominant nanosheets. Further studies would be required to characterize the influences of peptoid length, sidechain interactions, and nanoscale assembly on amide bond isomerization. It is worth emphasizing that the sample preparation procedures for B28 nanosheet and amorphous control samples yield differing degrees of protonation in the hydrophilic sidechains which may impact chain conformation and propensity for amide bond isomerization.

Until now, extended, linear molecular conformations in peptides and peptide-mimicking materials have always assumed an all-*trans* configuration along the backbone. Based on previous experimentation, we believe B28 monomers adopt extended conformations within nanosheets [1]. Therefore we simulated B28 monomers with all-*cis* and all-*trans* backbones, the results of which indicate that a low energy, all-*cis* state in which the molecule maintains overall linearity and sequestration of hydrophilic and hydrophobic sidechains is possible (Figure 5). Interestingly, *cis* Σ-strand corresponds to a shorter molecular length and would promote more compact arrangements of hydrophobic residues within nanosheet cores.

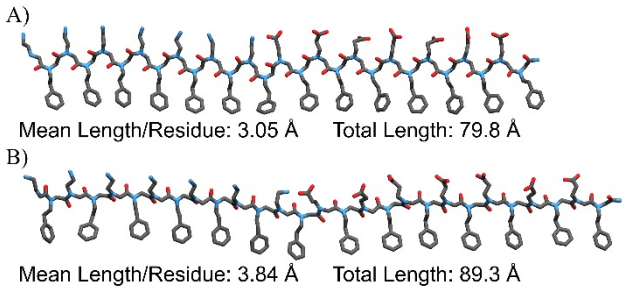

Figure 5. A) *Cis* Σ-strand configuration. B) *Trans* Σ-strand configuration. Length/residue and total molecular length values were obtained through molecular dynamics simulation of peptoid nanosheets.

In conclusion, the NMR data presented here show evidence of site-dependent contribution of the *cis* configuration in backbone amide bonds of monomer units within peptoid B28 nanosheets. In the center of the amino block, NMR reveals a predominantly *cis* configuration. In contrast, at the junction of the two charged blocks we observe a more even distribution of *cis* and *trans*. Additionally, PITHIRDS-CT measurements on unassembled B28 are consistent with previous predictions that solvated peptoid chains are primarily in the *trans* configuration. These results indicate that our findings have not altered our understanding of peptoid biology but rather our understanding of the energetics involved in peptoid nanostructures. Moving forward, observation of backbone amide bond isomerization within B28 nanosheets motivates a re-evaluation of the B28 molecular conformation in the short term; and for long-term development of peptoid nanostructure, shows that backbone isomerization must needs be taken into account. The previously proposed Σ-strand model assumed an all-*trans* configuration of the backbone amide bond because no experimental constraint on this degree of freedom existed at the time. The work presented here provides necessary groundwork to begin an overhaul of the B28 brickwork model, new insights into folding energetics of an entire class of synthetic biomaterials, and shows the efficacy of solid-state NMR in probing this new phenomenon.[21]

ASSOCIATED CONTENT

Supporting Information

The Supporting Information is available free of charge on the ACS Publications website.

Materials, synthesis procedure, and references for production of peptoid B28 nanosheets (PDF)

AUTHOR INFORMATION

Corresponding Authors

*anant.paravastu@chbe.gatech.edu
*rnzuckermann@lbl.gov

Notes

The authors declare no competing financial interests.

ACKNOWLEDGMENT

This synthesis and modeling work was funded by the Defense Threat Reduction Agency under Contract No. DTRA10027-15875 and the DARPA Fold F(x) program. Work at the Molecular Foundry was supported by the Office of Science, Office of Basic Energy Sciences, of the U.S. Department of Energy under Contract No. DE-AC02-05CH11231.

The authors acknowledge the use of NMR instruments at the NMR center at the Georgia Institute of Technology. We are grateful to Kong M. Wong for assistance with the SPINEVOLUTION simulations of nuclear spin dynamics.

REFERENCES

(1) Nam, K. T.; Shelby, S. A.; Choi, P. H.; Marciel, A. B.; Chen, R.; Tan, L.; Chu, T. K.; Mesch, R. A.; Lee, B. C.; Connoly, M. D.; Kisielowski, C.; Zuckermann, R. N. Free-floating Ultrathin Two-Dimensional Crystals from Sequence-Specific Peptoid Polymers. *Nat. Mater.* **2010**, 9, 454-460.

(2) Seurynck, S. L.; Patch, J. A.; Barron, A. E. Simple, Helical Peptoid Analogs of Lung Surfactant Protein B. *Chem. Biol*. **2005**, 12, 77-88.

(3) Wu, C. W.; Seurynck, S. L.; Lee, K. Y. C.; Barron, A. E. Helical Peptoid Mimics of Lung Surfactant Protein C. *Chem. Biol.* **2003**, 10, 1057-1063.

(4) Robertson, E. J.; Battigelli, A.; Proulx, C.; Mannige, R. V.; Haxton, T. K.; Yun, L.; Whitelam, S.; Zuckermann, R. N. Design, Synthesis, Assembly, and Engineering of Peptoid Nanosheets. *Acc. Chem. Res.* **2016**, 49, 379-389.

(5) Knight, A. S.; Zhou, E. Y.; Francis, M. B.; Zuckermann, R. N. Sequence Programmable Peptoid Polymers for Diverse Materials Applications. *Adv. Mater.* **2015**, 27, 5665-5691.

(6) Mirijanian, D. T.; Mannige, R. V.; Zuckermann, R. N.; Whitelam, S. Development and Use of an Atomistic CHARMM-Based Forcefield for Peptoid Simulation. *J. Comput. Chem.* **2014**, 35, 360-370.

(7) Sui, Q.; Borchardt, D.; Rabenstein, D. L. Kinetics and Equilibria of Cis/Trans Isomerization of Backbone Amide Bonds in Peptoids. *J. Am. Chem. Soc*. **2007**, 129, 12042-12048.

(8) Tycko, R. Symmetry-Based Constant-Time Homonuclear Dipolar Recoupling in Solid State NMR. *J. Chem. Phys.* **2007**, 126, 064506/1-9.

(9) Mannige, R. V.; Haxton, T. K.; Proulx, C.; Robertson, E. J.; Battigelli, A.; Butterfoss, G. L.; Zuckermann, R. N.; Whitelam, S. Peptoid Nanosheets Exhibit a New Secondary-Structure Motif. *Nature.* **2015**, 526, 415-420.

(10) Cormier, A. R.; Pang, X.; Zimmerman, M. I.; Zhou, H. X.; Paravastu, A. K. Molecular Structure of RADA16-I Designer Self-Assembling Peptide Nanofibers. *ACS Nano.* **2013**, 7, 7562-7572.

(11) Balbach, J. J.; Petkova, A. T.; Oyler, N. A.; Antzutkin, O. N.; Gordon, D. J.; Meredith, S. C.; Tycko, R. Supramolecular Structure in Full-Length Alzheimer's Beta-Amyloid Fibrils: Evidence for a Parallel Beta-Sheet Organization from Solid-State Nuclear Magnetic Resonance. *Biophys. J.* **2002**, 83, 1205-1216.

(12) Miller, Y.; Ma, B.; Nussinov, R. Polymorphism in Alzheimer's A-Beta Amyloid Organization Reflects Conformational Selection in a Rugged Energy Landscape. *Chem. Rev.* **2010**, 110, 4820-4838.

(13) Tycko, R.; Wickner, R. B. Molecular Structures of Amyloid and Prion Fibrils: Consensus Versus Controversy. *Acc. Chem. Res.* **2013**, 46, 1487-1496.

(14) Zujovic, Z.; Webber, A. L.; Travas-Sejdic, J.; Brown, S. P. Self-Assembled Oligoanilinic Nanosheets: Molecular Structure Revealed by Solid-State NMR Spectroscopy. *Macromolecules*. **2015**, 48, 8838-8843.

(15) Leclaire, J.; Poisson, G.; Ziarelli, F.; Pepe, G.; Fotiadu, F.; Paruzzo, F. M.; Rossini, A. J.; Dumez, J.; Elena-Herrmann, B.; Emsley, L. Structure Elucidation of a Complex CO_2-based Organic Framework Material by NMR Crystallography. *Chem. Sci.* **2016**, 7, 4379-4390.

(16) Fenniri, H.; Tikhomirov, G. A.; Brouwer, D. H.; Bouatra, S.; Bakkari, M. E.; Yan, Z.; Cho, J.; Yamakazi, T. High Field Solid-State NMR Spectroscopy Investigation of ^{15}N-Labeled Rosette Nanotubes: Hydrogen Bond Network and Channel-Bound Water. *J. Am. Chem. Soc.* **2016**, 138, 6115-6118.

(17) Simmons, T. J.; Mortimer, J. C.; Bernardinelli, O. D.; Poppler, A.; Brown, S. P.; deAzevedo, E. R.; Dupree, R.; Dupree, P. Folding of Xylan onto Cellulose Fibrils in Plant Cell Walls Revealed by Solid-State NMR. *Nat. Commun.* **2016**, 7.

(18) Reddy, G. N. M.; Huqi, A.; Iuga, D.; Sakurai, S.; Marsh, A.; Davis, J. T.; Masiero, S.; Brown, S. P. Co-existence of Distinct Supramolecular Assemblies in Solution and in the Solid State. *Chem. – Eur. J.* **2017**, 23, 2315-2322.

(19) Jaroniec, C. P.; Tounge, B. A.; Rienstra, C. M.; Herzfeld, J.; Griffin, R. G. Recoupling of Heteronuclear Dipolar Interactions with Rotational-Echo Double-Resonance at High Magic-Angle Spinning Frequencies. *J. Magn. Reson.* **2000**, 146, 132-139.

(20) Veshtort, M; Griffin, R. G. SPINEVOLUTION: A Powerful Tool for the Simulation of Solid and Liquid-State NMR Experiments. *J. Magn. Reson.* **2006**, 178, 248-282.

(21) Edison, J. R.; Spencer, R. K.; Butterfoss, G. L.; Hudson, B. C.; Hochbaum, A. I.; Paravastu, A. K.; Zuckermann, R. N.; Whitelam, S. Conformations of Peptoids in Nanosheets Result from the Interplay of Backbone Energetics and Intermolecular Interactions.

Proc. Natl. Acad. Sci. U. S. A. **2018**, DOI: 10.1073/pnas.1800397115.